PLEA 2020 A CORUÑA
Planning Post Carbon Cities

The effect of street grid form and orientation on urban wind flows and pedestrian thermal comfort

YARA AYYAD[1,2], STEVE SHARPLES[1]

[1]University of Liverpool, Liverpool, UK
[2]Al-Ahliyya Amman University, Amman, Jordan

ABSTRACT: Rapid urbanisation puts pressure on urban planning to create layouts that are sustainable, healthy and thermally comfortable for urban occupants. This study explores the influence of street grid form, as a single aspect of the urban layout, on wind flow, solar access and thermal stress in a hot climate. Four street scenarios based in Amman, Jordan were simulated under the same climatic conditions using the CFD modelling software Envi-MET. The analysis included different orientations for the designed grids to assess the effect of sun angle and wind direction. The results were compared in terms of average wind speed and physiological equivalent temperature (PET). Although wind speeds were found to change greatly for different orientations, PET was more sensitive to the different grid geometries rather than their orientation.
KEYWORDS: outdoor thermal comfort, Envi-MET, wind flow, urban layout, physiological equivalent temperature.

1. INTRODUCTION

Industrial, technological and economic growth in recent decades has led to a large increase in the world's population, with a projected global population by 2050 of 9.7 billion [1]. Most people will live in cities, creating problems of overcrowding, pollution and poor outdoor urban environments. Better informed and more sustainable planning might help improve comfort conditions for urban pedestrians as they move around city centres. This study explores how different street grid systems, as a single aspect of urban layout, can affect wind flow and thermal stress. Four scenarios were simulated under the same climatic conditions in the CFD modelling software Envi-MET. The analysis included two different street orientations to assess the effect on solar access, wind speed and wind direction. The results were compared in terms of average wind speed and the thermal comfort index physiological equivalent temperature (PET).

2. BACKGROUND

Designing an urban space that considers the wellbeing of its occupants goes through several stages, starting with the design phase and followed by the testing phase. Testing can be performed using the CFD modelling software Envi-MET— an urban modelling software that assesses the interaction between the selected site's microclimate and its built environment [2-5]. The impact of the generated microclimate on the thermal comfort of pedestrians can be assessed using the physiological equivalent temperature (PET) [6]. Unlike some other comfort metrics, PET values are influenced by local wind speeds and solar radiation conditions [7]. PET groups include 8-13^{o}C (cold); 18-23^{o}C (comfortable); 23-29^{o}C (slightly warm); 29-35^{o}C (warm); 35-41^{o}C (hot) and >41^{o}C (very hot).

3. METHODOLOGY.

The study site was Amman in Jordan, which has a climate of long hot summers and short cool winters. Four common urban layouts (three grid and one radial) on a 150 x 150m plot were modelled to quantify the effect of street grid form and street orientation on wind flow and PET (Fig. 1). The grids were simulated twice, once with streets running north to south and, by rotating the grid by 45° counter-clockwise, with the streets running NE-SW, creating two different wind directions. The data were extracted based on a human height of 1.75m.

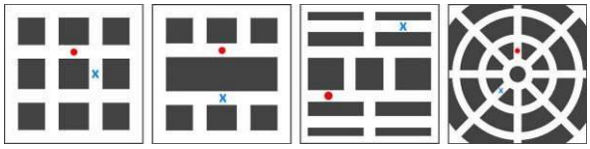

*Figure 1: Grid layouts A (left) to D (right), receptor 1 is shown as a red dot and receptor 2 as a blue cross **X**.*

All the Envi-MET inputs, apart from the grid layout, were kept the same: a building height to street width ratio of 1; the buildings' cladding material was white limestone (the most common choice in Jordan); street albedo was 10% (asphalt); and the dominant wind direction was westerly for all the layouts. The simulation results were compared in terms of wind speed distribution for each layout at 11:00 am, and PET thermal comfort over a 24-hour period for the two street receptors. The simulation date was 23rd September, with a minimum air temperature of 18°C, a maximum of 30°C, a 4 m/s starting wind speed, a minimum relative humidity of 50% and a maximum of 70%.

4. RESULTS AND DISCUSSION

The layouts were labelled from A-D and each orientation was given the number 1 for 45° orientation from the North and 2 for 0° orientation from the North. For each of the layouts, wind behaviour analysis was performed in terms of the speed and flow.

4.1 Street grid layout A

For the 45° direction from North layout, the wind enters the plot at an incidence angle of 45°, creating a flow separation when it reaches the sharp edge of the buildings. Vortices are formed in the cavity zone at the rear side façades of the buildings due to the lower surface pressures, causing wind speeds to reduce significantly compared to the mean flow in streets. As the wind flow progresses across the plot, a helical wind pattern is created throughout the streets - this phenomenon is the vector sum of the vortices and the channelling flows created by the external wind flow. Fig. 2 indicates the flow patterns, although the figure is too small to flows and speeds clearly.

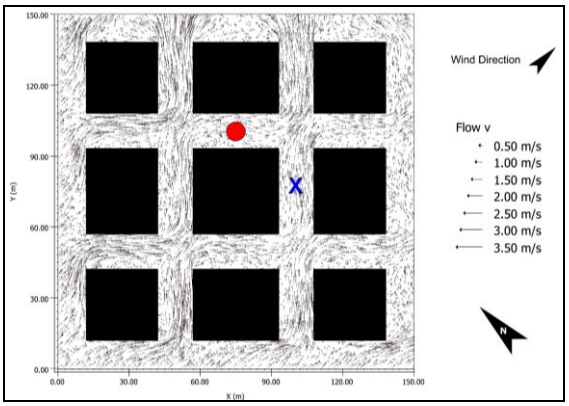

Figure 2: Wind flows and speeds for scenario A.1.

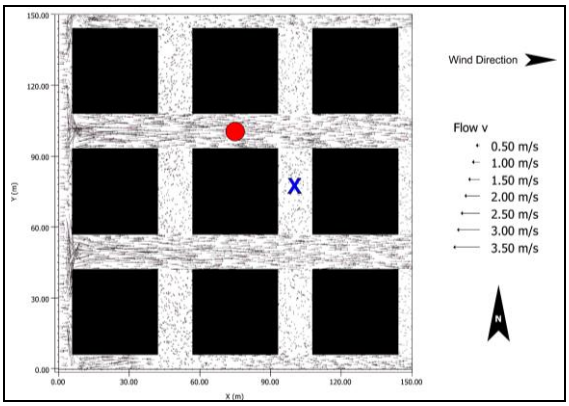

Figure 3: Wind flows and speeds for scenario A.2.

For scenario A.2, the wind enters the plot at 0° incidence angle, creating a channelling flow (Fig. 3). This flow produces a high pressure in the streets that are oriented in the flow path, which in turn, restricts the wind flow into the streets perpendicular to the flow. The high wind speed flow coming from the West in the West-East oriented streets create low velocity corner vortices in North-South streets. In the North-South streets, two vortices are created with opposite rotation directions, but because they have low velocity, they do not affect each other's flows. Scenario A.2 shows a higher percentage of higher wind speed than scenario A.1 (Fig. 4), but also a high percentage of low wind speed. Scenario A.1, with its more even distribution of wind speeds, has a better chance of providing comfort for pedestrians. Fig. 5 shows the range of PET values for the two receptors and the two wind direction scenarios A.1 and A.2. The dashed lines are the upper (23°C) and lower (18°C) PET values for comfort.

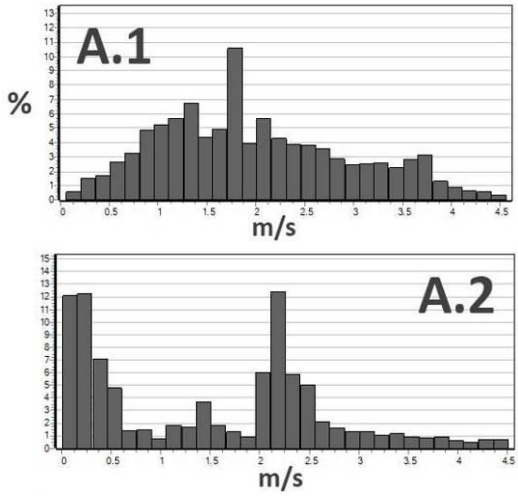

Figure 4: Wind speed distribution (%) for A.1 and A.2.

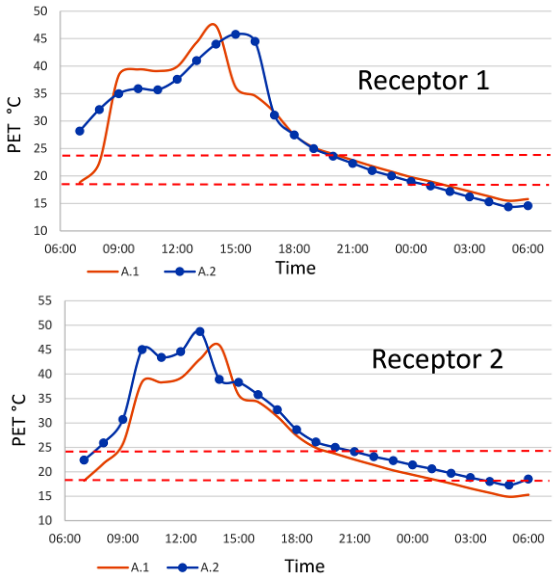

Figure 5: PET for receptors 1 and 2 for scenarios A.1 and A.2

Scenario A.2 has higher PET values than scenario A.1 during the early hours of the day and later on between the hours of 15:00 and sunset, the raise in PET values in this situation is due to the location of receptor 1, where it is situated on the west-east axis with no shading from the morning and evening sun, the opposite can be seen in A.1, where higher PET

levels were recorded during midday, due to the location of the receptor on the northern western-southern eastern axis which means it would not be shaded during the high sun from the south. The change of orientation of the plot changed the areas that sun would reach in different times of the day, and when inspecting the shadows casted by the buildings for both of the scenarios, it was concluded that scenario A.1 have the least time duration of direct sun radiation.

4.2. Street grid layout B

For scenario B.1 a flow separation occurs when the wind strikes the SW corner of the buildings, causing vortices to form in the cavity zone located at the rear of the buildings, where wind speeds are lower than the rest of the plot (Fig. 6). As wind flow enters the plot, it gets disturbed by the central attached building row and forms a flow that gets fed by the wind coming from the detached buildings and maintains high speeds. The wind flow is strong when it enters the street on the leeward side of the row buildings, however, it gets weaker as it loses its intensity moving forward due to its flow direction that allows flow separation when it hits the edges of the detached buildings.

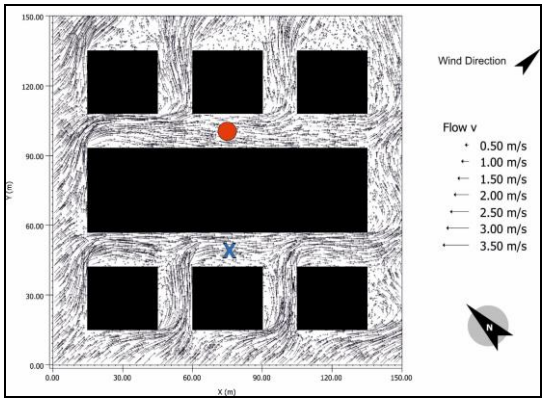

Figure 6: Wind flows and speeds for scenario B.1.

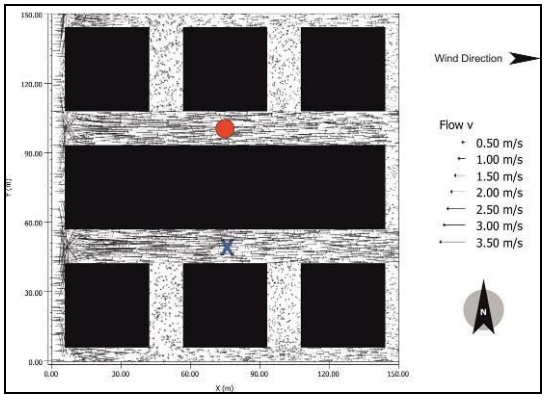

Figure 7: Wind flows and speeds for scenario B.2.

With scenario B.2 (Fig. 7) the wind is channelled along the W-E streets and the constriction increases the wind speeds to values slightly higher than scenario A.2. The high intensity of the channelled flows prevents strong flows entering the N-S streets, creating very low wind speeds. This is reflected in the high percentage frequency of low winds shown for scenario B.2 in Fig. 8, while B.1 shows a much better distribution (13% of wind speeds >2 m/s).

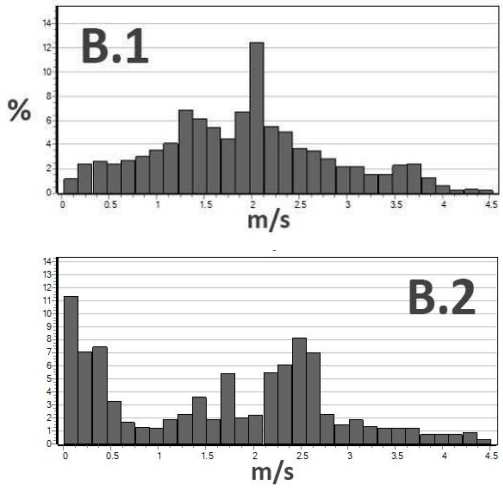

Figure 8: Wind speed distribution (%) for B.1 and B.2.

PET values in B1.1 and B.2 range from slightly cool to very hot and are heavily affected by solar access. The peak in PET for both receptors in Fig. 9, between 18:00 and 06:00, reflects the direct solar irradiation in the day. Wind speeds at both receptors were very similar, giving close night-time PET values. Daytime PET values are much higher in the more open layout of B.1 and B.2. The dashed lines are the upper (23°C) and lower (18°C) PET values for comfort.

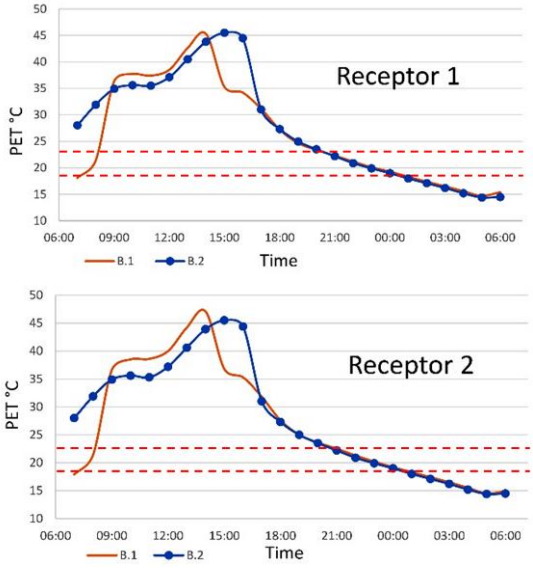

Figure 9: PET for receptors 1 and 2 for scenarios B.1 and B.2

4.3 Street grid layout C

The geometry in scenario C.1 introduces the effect of linear buildings against a cluster of square buildings. Fig. 10 shows wind flow enters SW corner of the plot and splits into two streams - the left stream, free of obstacles, accelerates while the right stream decelerates. Wind speeds increases in the

between the linear buildings compared to the big cluster of buildings in the middle of the plot. This is explained by the size of the cavity area cast by the bigger cluster of buildings where vortices are formed, and wind speed is reduced. Low wind speed can be seen in the NE corner due to the strong wind flow coming from street opening, which gets reinforced by the helical vortices from the adjacent canyons, all of this create strong pressures that prevent strong wind flows into the receptor 2 location.

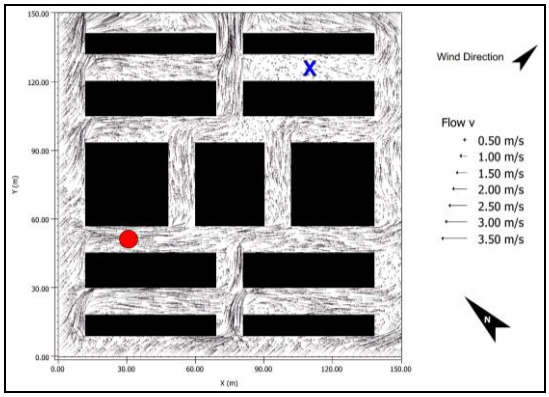

Figure 10: Wind flows and speeds for scenario C.1.

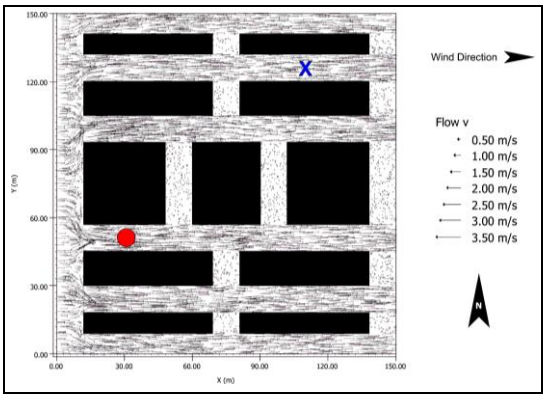

Figure 11: Wind flows and speeds for scenario C.2.

For scenario C.2, the west wind is channelled and accelerated through the West-East streets, which limits wind penetration into the N-S streets (Fig. 11). Low speed vortices are formed in the shorter N-S streets, while longer N-S streets have two vortices forming from each end with opposite rotations. The C.2 orientation may raise the overall wind speed, but it produces areas with very low air movement. The percentage frequency distribution of wind speeds across the site for C.1 is almost normal, with a spike around 2.2 m/s (Fig. 12). In scenario C.2 the distribution clusters tightly around higher speeds (2 to 2.5 m/s). However, the distribution also shows a higher count of low speeds than scenario C.1.

Fig. 13 shows the hourly PET values levels for C.1 and C.2. Daytime PETs range from comfortable to very hot, and are heavily influenced by incident solar radiation, and orientation is crucial in determining the site's sunlit and shaded areas. With receptors 1 and 2, the PET values for scenario C.2 spike at 09:00 and again before sundown at 17:00. The sun directly these receptors when in the east and west (i.e. morning and late afternoon). However, these receptors are shaded when the sun is between SE and SW (09:00-14:00). PET values drop drastically at night due to the lack of solar radiation.

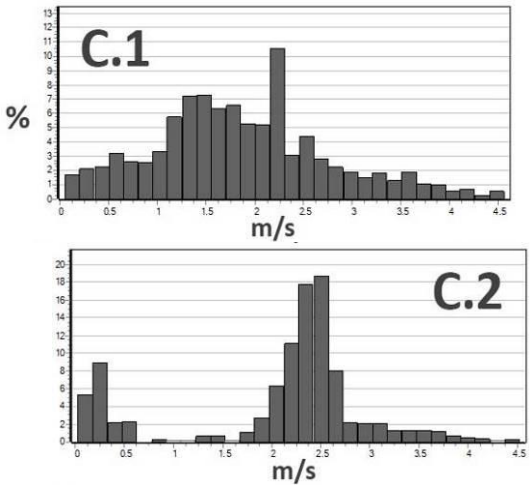

Figure 12: Wind speed distribution (%) for C.1 and C.2.

The night-time PET levels vary from comfortable to slightly cool and show the effect of wind speed. Receptor 2 has a higher PET value for scenario C.1 than C.2 due to C.1's lower wind speeds, while receptor 1 has similar C.1 and C.2 PET levels due to similar wind speed values. The dashed lines are the upper (23°C) and lower (18°C) PET values for comfort.

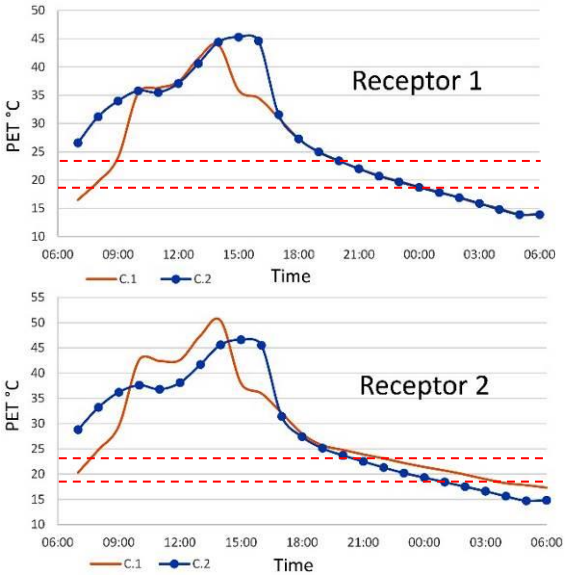

Figure 12: PET for receptors 1 and 2, scenarios C.1 and C.2

4.4 Street grid layout D

A radial street geometry was tested to see if it offered any advantages over the grid layouts. Fig. 14 for the rotated plan (D.1) shows wind entering the plot from the SW corner and slowing as it progresses along the street due to a lack of reinforcing flows from other streets. The main wind flow passes

receptor 2 with a low velocity to reach the centre of the plot before splitting into two flows. These two flows have higher wind speed values because they are joined by two streams passing through the W-E and N-S streets. Wind speeds across the plot average 0.15 to 1.4 m/s compared to the 4 m/s initial speed.

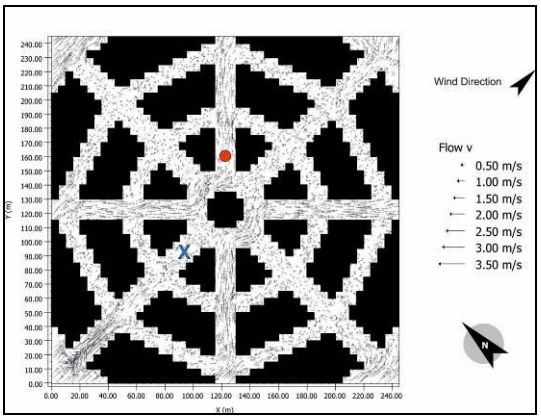

Figure 13: Wind flow for scenario D.1.

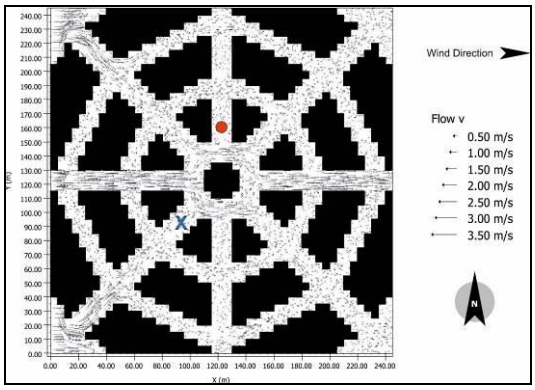

Figure 14: Wind flow for scenario D.2.

For scenario D.2 (Fig. 15) wind enters the plot from the west and maintains its speed along the street until it reaches the centre of the plot, then the flow divides into two streams moving around the centre of the plot and exiting through the end of the west oriented street. For scenario D.1 the flow leaves the plot through two streets passing through the north oriented and west oriented streets; but in Scenario D.2 the flow separates and then recombines in the same line of motion. This might have happened as a shortcoming in Envi-MET, which read the edges of the building as small ridges rather than a continuous line. The average wind speeds inside the plot are low, from 0.1-1.25 m/s.

The wind speed percentage distributions (Fig. 16) show that for the radial plan most speeds are lower than for the grid layouts. Scenario D.1 did have some areas with wind speeds of 0.5-1.5 m/s, but the majority of speeds for scenario D.2 were in the range 0 to 0.75 m/s. Both scenarios show low air flow, which raises the risk of poor pollutant dispersion.

Fig. 17 shows the PET values over the 24 hours of simulation, ranging from slightly warm to slightly cool during the night, and from slightly warm to very hot during the day. The radial layout allows the sun to shine on the location of the receptors at various times during the day, and this produces spikes in the PET curves as the receptors are irradiated. This is more apparent for receptor 2 due to its location.

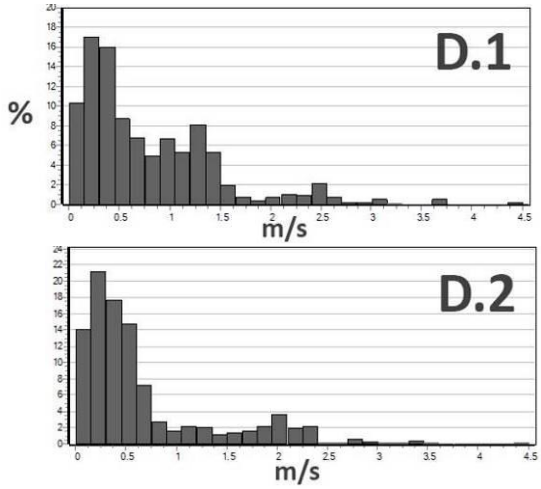

Figure 15: Wind speed distribution (%) for D.1 and D.2.

PET values for scenario D.1 are noticeably higher than for scenario D.2 between 06:00-09:00 and 15:00-18:00. This is due to its location being on the West-East axis, where direct sun reaches the receptors in the morning and evening. Receptor 1 shows the same tendencies as receptor 2 where there is a spike when the sun reaches the location. However, the location of the receptor limited the morning and evening solar access, and this resulted in high PET levels from 10:00 to 14:00 in D.1 and from 10:00 to 13:00 in D.2. The dashed lines are the upper (23°C) and lower (18°C) PET values for comfort.

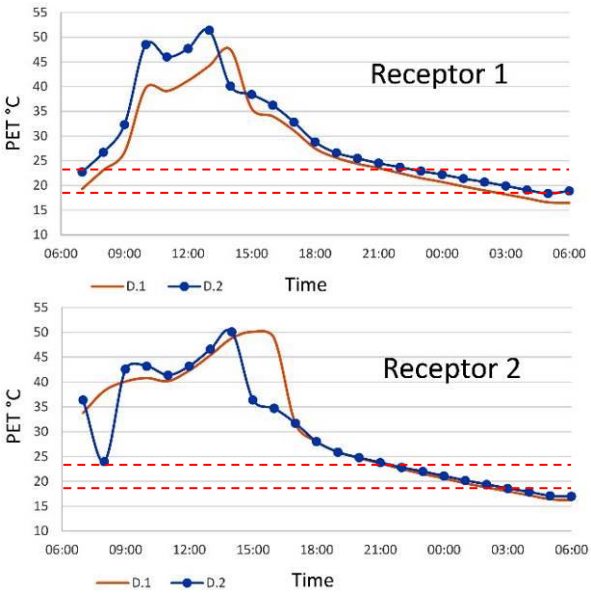

Figure 16: PET for receptors 1 and 2, scenarios D.1 and D.2

PET levels for both scenarios are reduced at night and have very close values, as was seen for all of the previous layouts. This can be explained by the close

night-time values of the meteorological factors - air temperature, wind speed, mean radiant temperature and relative humidity. It has been noticed that some of the meteorological factors, like the air temperature and relative humidity, are difficult to influence in an urban layout through geometrical modification. However, other meteorological factors, like wind speed and mean radiant temperature, vary significantly from one urban form to the other, which creates the big difference in PET values at day and the small difference at night.

4. CONCLUSION

Street grid layouts are comprised of a multitude of variables that impact upon their environmental performance. These included orientation, wind direction, albedo and height to width ratio. For the sake of containing the quantity of results in this study, some variables were assumed as having fixed values for each grid. The street grid analysis covered the geometrical composition of four designs - three orthogonal grids and one radial grid. The building properties and starting meteorological conditions for every grid were the same to ensure all results reflected changes only due to the grid layout and the wind direction.

The street grid analysis showed interesting results for the different layouts. Wind speed was affected greatly by the change of orientation, where the 45° counter-clockwise rotation from North showed a major improvement in wind flow distributions. However, the change in orientation did not play a key role in changing PET levels, even though the change in orientation changed the shadow patterns. The main reason behind the rise and fall of PET levels was the geometry of the plot, whether it was rotated from the original orientation or not. Understanding the geometry of the site is a key component in determining the thermal stress on the human body, Jiang, et al, 2020, concluded similar findings with their study on parallel and staggered urban layouts, where the staggered layout performed better based on the shape and spacing they proposed. Table 1 shows the percentage of the 150 x 150m plot area that experienced low wind speeds (0 to 0.5 m/s) for the various geometrical layouts.

Table 1: Percentage area of plot with wind speeds 0-0.5 m/s

LAYOUTS	A		B		C		D		E	
SCENARIOS	A.1	A.2	B.1	B.2	C.1	C.2	D.1	D.2	E.1	E.2
AREA PERCENTAGE	6%	36%	8%	29%	9%	18%	52%	68%	42%	60%

All of the scenarios 1, with a 45° counter-clockwise rotation from the north, showed improved wind flow results when compared to scenarios 2 with no turn from the north. Layout A scenario 1 showed better results across all layouts and scenarios with only 6% of the plot area having low wind speeds, while layout D showed the worst results across all layouts due to its curved streets that obstructed wind flow, with 68% of plot area having low wind speeds.

Table 2 shows the average PET values for all the layouts over the 24 period of simulations.

Table 2: Average PET values for all layouts.

LAYOUTS	A		B		C		D		E	
SCENARIOS	A.1	A.2	B.1	B.2	C.1	C.2	D.1	D.2	E.1	E.2
PET	26.1	27.2	26.6	27.6	26.7	28.3	28.2	29.3	28.4	29.6

The average PET values shown in Table 2 do not convey how well the layouts present their comfort level, but rather they show how in the same layout the different orientation (scenarios 1 and 2) shifts the comfort levels. An increase in PET values is noticed in all of the layouts in scenario 2, which is caused by the North-South orientation streets that receive the highest levels of solar radiation throughout the day. In terms of the most favourable range of PET values for comfort over the 24 hours of the studied day, the simple layout A (a 3 x 3 array of square buildings) had slightly better PET values than the other grid layouts.

REFERENCES

1. United Nations, (2019). World population prospects: The 2019 revision, New York, UN Population Division. https://population.un.org/wpp/Publications/Files/WPP2019_Highlights.pdf

2. Bruse, M., (2019), ENVI-met. https://www.envi-met.com/

3. Ayyad Y.N. and S. Sharples, (2019). Envi-MET validation and sensitivity analysis using field measurements in a hot arid climate. In *Proc. SBE19 Conference,* Cardiff, 24-25 September 2019. IOP Conference Series: Earth Environ. Sci., **329** 012040

4. Wasim Yahia, M.W. and E. Johansson, (2013). Influence of urban planning regulations on the microclimate in a hot dry climate: The example of Damascus, Syria. *J Hous and the Built Environ*, **28**: p.51-65

5. Hamdan D.M.A. and F.L. Oliveira, (2019). The impact of urban design elements on microclimate in hot arid climatic conditions: Al Ain City, UAE. *Energy and Buildings*, **200**: p.86-103.

6. Hoppe, P., (1999). The physiological equivalent temperature – a universal index for the biometeorological assessment of the thermal environment. *Int J Biometeorol*, **43**(2): p. 71-75.

7. Lee, H., H. Mayer, and W. Kuttler, (2019). To what extent does the air flow initialisation of the ENVI-met model affect human heat stress simulated in a common street canyon? *Int J Biometeorol*, **63**: p. 73-81.

8. Jiang, Y., C. Wu and M. Teng, (2020). Impact of residential building layouts on microclimate in a high temperature and high humidity region. *Sustainablity,* **12**(3), article no. 1046.